SUPPORTING INFORMATION

Highly Water-dispersible and Antibacterial Magnetic Clay Nanotubes Functionalized with Polyelectrolyte Brushes: High Adsorption Capacity and Selectivity Toward Heparin in Batch and Continuous System

Mohammad Arshadi[†], Hamed Eskandarloo[†], Mojtaba Enayati, Mary Godec, Alireza Abbaspourrad*

Department of Food Science, College of Agriculture & Life Sciences, Cornell University, 243 Stocking Hall, Ithaca, NY 14853, USA

*Corresponding author:

E-mail address: alireza@cornell.edu

Tel.: (607) 255-2923

[†]These authors contributed equally to this work.

To measure monomer conversions at different times, approximately 100 μL of the sample was dissolved in D_2O and filtered with a 0.22 μm nylon membrane prior to acquisition of the ^{1}H-NMR spectra. The conversion was calculated by comparison between the integral of the dimethyl sulfoxide (DMSO) peak (which was added to the polymerization mixture as a reference before polymerization) with that of the remaining monomer. Based on the integral of the (b) hydrogens at 5.60–6.00 ppm compared to the hydrogens of DMSO at 2.75 ppm, which the integral value was set at 0.66 (Figure S1) in the ^{1}H-NMR spectra, a monomer conversion of 39% was determined after 10 min, 74% after 30 min, and 93% after 60 min of the polymerization reaction, according to Eq. S1.

Conversion (%) = {1 − [[(peak area of b hydrogen)/(peak area of DMSO)]× 0.66]} × 100   (Eq. S1)
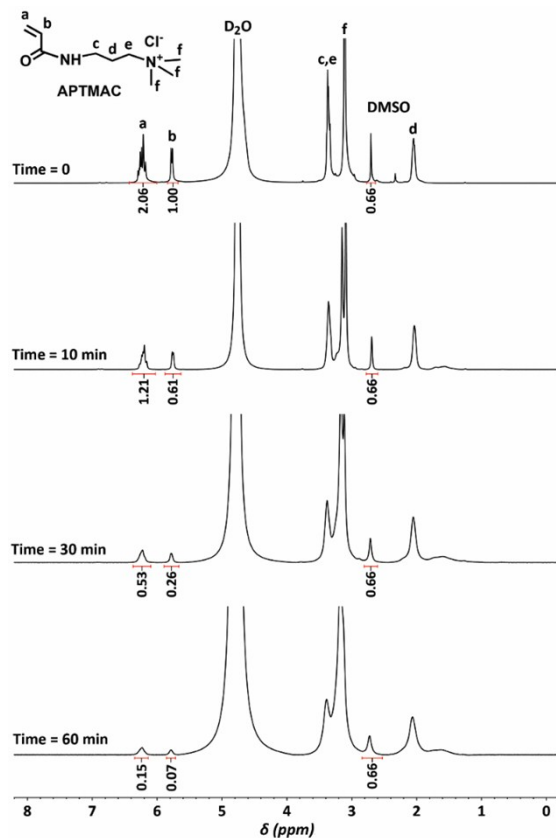
Figure S1. 500 MHz ^{1}H-NMR spectra of the reaction mixture at different times for the surface initiated Cu(0)-mediated RDRP of APTMAC from the HNT@Fe-Br.
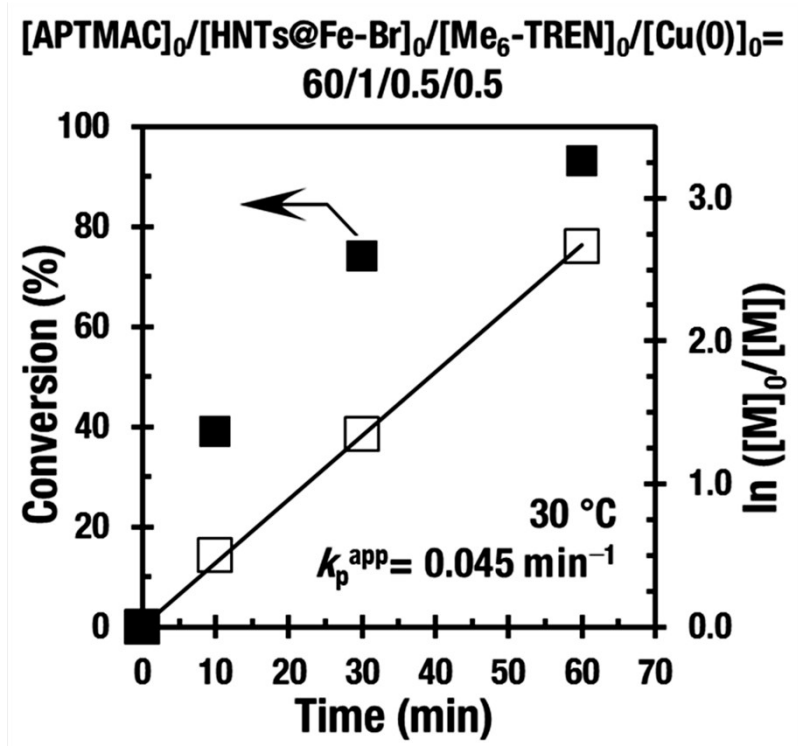
Figure S2: Kinetics of the Cu(0)-mediated RDRP reaction of APTMAC onto the surface of the HNTs@Fe-Br.

Figure S3. Breakthrough test set-up using a 3 mL syringe filled with 100 mg of HNTs@Fe-PAPTMAC.
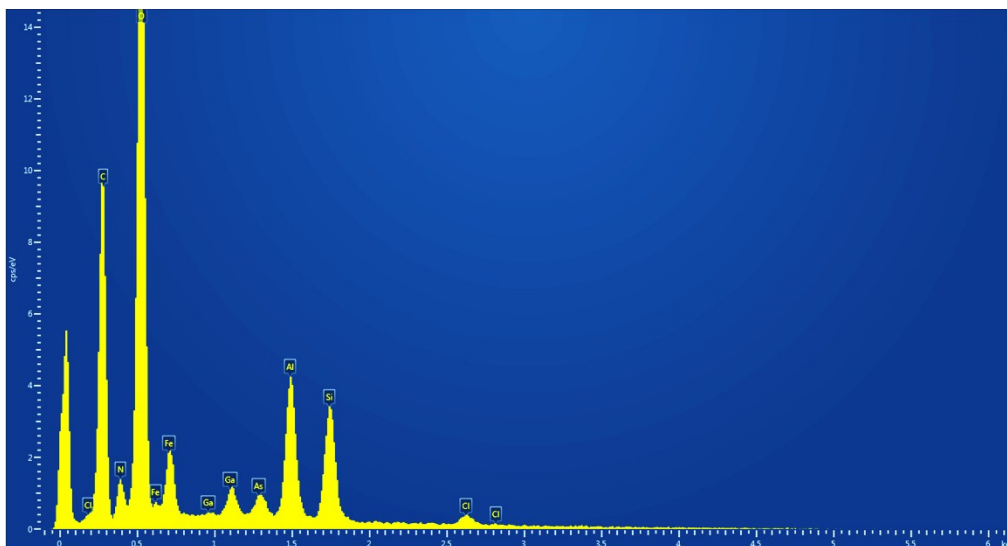
Figure S4. Energy dispersive x-ray spectroscopy (EDS) graph of the HNTs@Fe-PAPTMAC (60 min) sample on a gallium arsenide (GaAs) wafer.

Table S1. Adsorption isotherm and kinetics equations.

Formula	Equation
Langmuir	$q_e = \dfrac{q_m K_L C_e}{1 + K_L C_e}$
Freundlich	$q_e = K_F C_e^{1/n}$
Pseudo-first-order	$q_t = q_e[1-exp(-k_1 t)]$
Pseudo-second-order	$q_t = k_2 q_e^2 t/1 + k_2 q_e t$
Weber-Morris	$q_t = k_{int} t^{1/2} + I$
Initial adsorption rate	$h = k_2 q_e^2$
Separation factor	$\alpha_{Anion}^{Heparin} = \dfrac{K_d^{Heparin}}{K_d^{Anion}}$

* q_e (mg g^{-1}) is the specific equilibrium amount of the adsorbate, C_e (mg L^{-1}) is the equilibrium concentration of the adsorbate, C_0 (mg L^{-1}) is the anion concentration, C_t (mg L^{-1}) is the outlet concentration at time t, V is the volume of the solution (L), m is the amount of adsorbent (g), q_m is the maximum adsorption capacity, and K (K_L and K_{LF}) (L mol^{-1}) and n are empirical constants that indicate the extent of adsorption and the adsorption effectiveness, respectively. The constant n gives an idea of the grade of heterogeneity in the distribution of energetic centers of the adsorbent's active sites and is related to the magnitude of the adsorption driving force. Therefore, high n values indicate a relatively uniform adsorbent surface, while a low n values indicate high adsorption at low solution concentrations and also the existence of a high proportion of high-energy active sites. I is a constant related to the thickness of the boundary layer.[1] k_1, k_2, and k_{int} are the adsorption rate constants of the first and second order kinetic and intra-particle diffusion models, in min^{-1}, (g (mg min)$^{-1}$), and mg g^{-1} min$^{-1/2}$, respectively. q_e and q_t in mg g^{-1}, are equilibrium adsorption uptake (at time $t = \infty$) and adsorption uptake (at time t), respectively.

Table S2. Characteristics of different adsorbents for heparin recovery reported in the literature.

Adsorbent	Adsorption capacity (mg/g)	Reference
Chitosan microspheres	75.70	2
Cross-linked chitosan microspheres	0.16	3
Quaternized chitosan/polystyrene beads	3.28	4
Activated charcoal	40	5
Hydroxyapatite	16.38	6
Poly(2-hydroxyethyl methacrylate) cryogel	270	7
Poly(acryloxyethyltrimethyl ammonium chloride)/SiO_2	121	8
HNTs@Fe-PAPTMAC	123.9	This work

Reference

(1) K.Ahmadi, M.Ghaedi, A.Ansari, *Spectrochim Acta A* 2015, **136**, 1441-1449.

(2) M. Guerrini, D. Beccati, Z. Shriver, A. Naggi, K. Viswanathan, A. Bisio, I. Capila, J. C. Lansing, S.; Guglieri, B.; Fraser, A. Al-Hakim, *Nat Biotechnol* 2008, **26 (6)**, 669-675.

(3) M. Guerrini, A. Bisio, G. Torri. *Semin Thromb Hemost* 2001, **27**, 473-482.

4) H. Eskandarloo, M. Godec, M. Arshadi, O. I. Padilla-Zakour, A. Abbaspourrad, *Chem Eng J* 2018, **348**, 399-408.

(5) C. Bett, K.; Grgac, D. Long, M. Karfunkle, D. A.; Keire, D. M.; Asher, L. A. Gregori, *AAPS J.* 2017, **19(3)**, 765-771.

(6) K. R. Holme, A. S. Perlin, *Carbohydr Res* 1989, **186**, 301-312.

(7) X. Wei, J. Duan, X. Xu, L.Zhang, *ACS Sustainable Chem Eng* 2017, **5**, 3195- 3203.

(8) K. Kaminski, K. Zazakowny, K. Szczubiałka, M.Nowakowska, *Biomacromolecules* 2008, **9**, 3127-3132.